



Universiteit
Leiden
The Netherlands

**Cobalt(II)-disulfide compounds with the unusual PF₂O₂- anion.
ligand-dependent redox conversion to a cobalt(III)-thiolate complex**

Jiang, F.; Marvelous, C.; Verschuur, A.C.; Siegler, M.A.; Teat, S.J.; Bouwman, E.

Citation

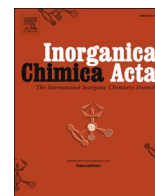
Jiang, F., Marvelous, C., Verschuur, A. C. S., M. A., Teat, S. J., & Bouwman, E. (2022). Cobalt(II)-disulfide compounds with the unusual PF₂O₂- anion. ligand-dependent redox conversion to a cobalt(III)-thiolate complex. *Inorganica Chimica Acta*, 535.
doi:10.1016/j.ica.2022.120880

Version: Publisher's Version

License: [Creative Commons CC BY 4.0 license](#)

Downloaded from: <https://hdl.handle.net/1887/3303532>

Note: To cite this publication please use the final published version (if applicable).



Cobalt(II)-disulfide compounds with the unusual PF_2O_2^- anion. ligand-dependent redox conversion to a cobalt(III)-thiolate complex

Feng Jiang^{a,1}, Christian Marvelous^{a,1}, Amaya C. Verschuur^a, Maxime A. Siegler^b, Simon J. Teat^c, Elisabeth Bouwman^{a,*}

^a Leiden Institute of Chemistry, Gorlaeus Laboratories, Leiden University, P.O. Box 9502, 2300 RA Leiden, the Netherlands

^b Department of Chemistry, Johns Hopkins University, 3400 N. Charles Street, Baltimore, MD 21218, United States

^c Advanced Light Source, Berkeley Laboratory, 1, Cyclotron Road, CA 94720, Berkeley, United States

ARTICLE INFO

Keywords:

Redox conversion
Cobalt(II) disulfide
Cobalt(III) thiolate

ABSTRACT

Herein we describe the synthesis of the cobalt(II) disulfide compounds $[\text{Co}^{\text{II}}_2(\text{L}^x\text{SSL}^x)(\mu\text{-PO}_2\text{F}_2)_2](\text{PF}_6)_2$ and $[\text{Co}^{\text{II}}_2(\text{L}^x\text{SSL}^x)(\text{NO}_3)_4]$ ($x = 1$: di-2-(bis(2-pyridylmethyl)amino)-ethyl disulfide; $x = 2$: di-2-((6-methyl-2-pyridylmethyl)(2-pyridylmethyl)amino)-ethyl disulfide). The crystal structures show the cobalt(II) centers in $[\text{Co}^{\text{II}}_2(\text{L}^x\text{SSL}^x)(\mu\text{-PO}_2\text{F}_2)_2](\text{PF}_6)_2$ to be in distorted octahedral geometries, whereas in $[\text{Co}^{\text{II}}_2(\text{L}^1\text{SSL}^1)(\text{NO}_3)_4]$ the geometries are distorted trigonal bipyramidal. The cobalt(II) centers in $[\text{Co}^{\text{II}}_2(\text{L}^x\text{SSL}^x)(\text{PO}_2\text{F}_2)_2](\text{PF}_6)_2$ are coordinated by three nitrogen and one sulfur donor atom of the disulfide ligand, and two oxygen atoms of two bridging difluoridophosphate anions. The cobalt(II) centers in $[\text{Co}^{\text{II}}_2(\text{L}^1\text{SSL}^1)(\text{NO}_3)_4]$ are coordinated by three nitrogen donors of the ligand and three oxygen atoms of one monodentate and one bidentate nitrate anion, the latter two oxygen atoms together occupying one of the equatorial sites of the trigonal bipyramid. It was found that the dinuclear compound $[\text{Co}^{\text{II}}_2(\text{L}^1\text{SSL}^1)(\text{PO}_2\text{F}_2)_2](\text{PF}_6)_2$ is stable as such in methanol and dichloromethane solution, but in acetonitrile redox conversion occurs forming the cobalt(III) thiolate compound $[\text{Co}^{\text{III}}(\text{L}^1\text{S})(\text{MeCN})_2]^{2+}$. The compound $[\text{Co}^{\text{II}}_2(\text{L}^1\text{SSL}^1)(\text{NO}_3)_4]$ and the disulfide compounds of the ligand L^2SSL^2 do not show this redox conversion and remain in the disulfide form in all investigated solvents.

1. Introduction

Electron-transfer reactions involving thiolate-disulfide interconversion occur in a number of biological processes and play fundamental roles in e.g. copper transport, regulation of gene expression, and protein folding and stability [1–4]. However, until now, the exact mechanism of these electron-transfer reactions in vivo is not well understood [2]. Understanding of the disulfide-thiolate redox reaction with transition metal ions such as cobalt, copper, or gold is also important for the study of metallodrugs, as these often are activated or deactivated through reduction by glutathione or other thiol groups in living tissue [5–7]. To gain more insight in the operation principle of the thiolate-disulfide redox reaction occurring in metalloenzymes or metalloproteins such as metallothionein Zn_7MT_3 [8–10], research efforts have been devoted to the synthesis of copper(II) thiolate compounds and the study of their redox interconversion to the corresponding copper(I) disulfide compounds [11–16]. So far, several triggers have been found to tune this

redox interconversion such as the pH of the solution [13,15], the presence or absence of halide ions [12,16], as well as the coordinating properties of solvents [14,15], and changes in temperature [14].

In the last few years, the study of the redox interconversion between metal thiolate and disulfide compounds has progressively moved from copper to other transition metal ions. The group of Duboc reported the electrochemical synthesis of a cobalt(III)-thiolate compound and its redox interconversion to the related cobalt(II)-disulfide compound induced by the removal of chloride anions [17]. Recently, our group presented the synthesis of a cobalt(III)-thiolate compound by the reaction of a disulfide ligand with certain cobalt(II) salts and the redox interconversion to the related cobalt(II)-disulfide compound triggered by the addition of chloride anions [18]. The group of Stack and our group reported the formation of the copper(I)-disulfide isomer upon dissolution of copper(II)-thiolate compounds in acetonitrile [14,15]. On the other hand, the group of Duboc reported the formation of an iron(III)-thiolate compound in the presence of acetonitrile or

* Corresponding author.

E-mail address: bouwman@lic.leidenuniv.nl (E. Bouwman).

¹ Equal contributions.

dimethylformamide [19]. Coordination of the solvent molecule thus seems to affect the formation of either the disulfide or the thiolate species, depending on the ligand as well as the metal ion.

In this manuscript, we report the formation of cobalt(II)-disulfide compounds with nitrate anions as well as the unusual PO_2F_2^- anion, and the conversion to a cobalt(III)-thiolate compound in acetonitrile for one of these dinuclear complexes.

2. Experimental

2.1. General procedures

All reagents were obtained from commercial sources and used as received unless noted otherwise. LiPO_2F_2 was purchased from ChemFish co. Ltd, China [20]. Acetonitrile and diethyl ether were obtained from a solvent dispenser (PureSolv 400). Dichloromethane and methanol were purchased from commercial vendors and stored on 3 Å molecular sieves. The synthesis of cobalt compounds was carried out using standard Schlenk-line techniques under a nitrogen atmosphere. ^1H NMR and ^{13}C NMR spectra were recorded on a Bruker 300 DPX spectrometer at room temperature. Mass spectra were recorded on a Finnigan Aqua mass spectrometer with electrospray ionization (ESI). IR spectra were acquired on a PerkinElmer UATR spectrum equipped with a single reflection diamond (scan range 400 cm^{-1} to 4000 cm^{-1} , resolution 4 cm^{-1}). UV–vis spectra were collected in solution using a transmission dip probe with variable path length on an Avantes Avaspec-2048 spectrometer with Avalight-DH-S-BAL light source. Solid state UV–vis spectra were collected using a reflection probe consisting of 7 fiber optics (6 light-fibers, 1 reading fiber) with a wavelength range of 200–2500 nm. During the measurements, the distance between the probe and the solid material is fixed using a reflectance probe holder and sample holder positioned on top of each other. The probe holder and the sample holder were covered by aluminium foil to prevent light entering the reading fiber. The measurements were corrected using a dark reference correction. Elemental analyses were performed by the Microanalytical Laboratory Kolbe in Germany.

2.2. Single crystal X-ray crystallography

For $[\text{Co}^{\text{II}}_2(\text{L}^1\text{SSL}^1)(\text{NO}_3)_4]$ and $[\text{Co}^{\text{II}}_2(\text{L}^1\text{SSL}^1)(\text{PO}_2\text{F}_2)_2](\text{PF}_6)_2$ the reflection intensities were measured at 110(2) K using a SuperNova diffractometer (equipped with Atlas detector) with Mo $K\alpha$ radiation ($\lambda = 0.71073\text{ \AA}$) under the program CrysAlisPro (Version CrysAlisPro 1.171.39.29c, Rigaku OD, 2017). The same program was used to refine the cell dimensions and for data reduction. The structure was solved with the program SHELXS-2014/7 and was refined on F^2 with SHELXL-2014/7 [21]. Numerical absorption correction based on Gaussian integration over a multifaceted crystal model was applied using CrysAlisPro. The temperature of the data collection was controlled using the system Cryojet (manufactured by Oxford Instruments). The H atoms were placed at calculated positions using the instructions AFIX 23 or AFIX 43 with isotropic displacement parameters having values 1.2 Ueq of the attached C atoms. The structures of $[\text{Co}^{\text{II}}_2(\text{L}^1\text{SSL}^1)(\text{NO}_3)_4]$ and $[\text{Co}^{\text{II}}_2(\text{L}^1\text{SSL}^1)(\text{PO}_2\text{F}_2)_2](\text{PF}_6)_2$ are partly disordered.

One of the coordinating nitrate anions in $[\text{Co}^{\text{II}}_2(\text{L}^1\text{SSL}^1)(\text{NO}_3)_4]$ is disordered over two orientations; the occupancy factor of the major component refines to 0.905(4). The crystal that was mounted on the diffractometer was also twinned with two components. The twin relationship corresponds to a twofold axis along the reciprocal c^* direction. The BASF scale factor refines to 0.3725(8).

The two PF_6^- counter ions in $[\text{Co}^{\text{II}}_2(\text{L}^1\text{SSL}^1)(\text{PO}_2\text{F}_2)_2](\text{PF}_6)_2$ are found to be disordered over either two or three orientations. All occupancy factors can be retrieved from the cif file. The asymmetric unit also contains about 3.3 lattice dichloromethane solvent molecules spread out over four different sites. One solvent molecule is found to be partially occupied with an occupancy factor refined to 0.923(2). Another solvent

molecule is found at a site of inversion symmetry, and is also partially occupied. The occupancy factor refines to 0.4146(17). The two species that bridge the two Co metal centers (Co1 and Co2) were identified as two difluoridophosphate counter ions. The occupancy factors of P1, O1, O2, F1, F2 and P2, O3, O4, F3, F4 were initially set to refine freely (before eventually being constrained to be equal to one), and their refined values (esd) were 0.980(3), 1.043(6), 1.040(6), 1.001(5), 1.002(5) and 0.980(3), 1.058(6), 1.046(6), 1.004(5), 1.011(5), respectively. A quick search on the CSD confirmed that the P – O and P – F bond distances from the literature are consistent with those found in this crystal structure.

The data for $[\text{Co}^{\text{II}}_2(\text{L}^2\text{SSL}^2)(\text{PO}_2\text{F}_2)_2](\text{PF}_6)_2$ were collected on a Bruker APEX II CCD diffractometer at the Advanced Light Source beamline 11.3.1 at Lawrence Berkeley National Laboratory from a silicon(111) monochromator ($T = 100\text{ K}$, $\lambda = 0.7749\text{ \AA}$). The crystal was taken directly from its solution, with a drop of Paratone-N oil and immediately put into the cold stream or dry N_2 on the goniometer. The structure was solved by direct methods and the refinement on F^2 and all further calculations were carried out with the SHELX-TL suite.

2.3. Synthesis of the Cobalt(II) compounds

$[\text{Co}^{\text{II}}_2(\text{L}^1\text{SSL}^1)(\text{PO}_2\text{F}_2)_2](\text{PF}_6)_2$.

The ligand L^1SSL^1 (0.20 mmol; 103.3 mg) was dissolved in 5 mL dry and degassed methanol, and then CoCl_2 (0.40 mmol; 51.9 mg) was added, giving a dark purple solution. After stirring for 30 min a purple suspension was obtained. Then, AgPF_6 (0.80 mmol; 202.3 mg) and LiPO_2F_2 (0.40 mmol; 43.1 mg) were added to the reaction mixture, resulting in a pink solution with a white precipitate. The obtained mixture was stirred for another 2 h, and filtered through celite, yielding a clear red solution. The obtained red solution was evaporated to 1 mL, to which 15 mL diethyl ether was added, yielding an oily material. This oily material was dissolved in dichloromethane; vapor diffusion of diethyl ether into this solution resulted in the formation of pink crystals. Yield: 64.0 mg, 0.06 mmol, 30%. Elemental analysis calcd (%) for $\text{C}_{28}\text{H}_{32}\text{Co}_2\text{F}_{16}\text{N}_6\text{O}_4\text{P}_4\text{S}_2$: C 29.86, H 2.86, N 7.46; Found: C 29.81, H 2.88, N 7.40. ESI-MS in acetonitrile: found (calcd) for $\frac{1}{2}[\text{M}-2\text{PF}_6-2\text{PO}_2\text{F}_2 + 4\text{MeCN}]^{2+}$ ($=[\text{Co}^{\text{III}}(\text{L}^1\text{S})(\text{MeCN})_2]^{2+}$) m/z 199.5 (199.5); $\frac{1}{2}[\text{M}-2\text{PF}_6]^+$ m/z 418.2 (418.0); $\frac{1}{2}[\text{M}-2\text{PF}_6 + 2\text{MeCN}]^+$ m/z 459.2 (459.0). UV–vis in acetonitrile at 1 mM [Co] concentration: 238 nm ($\epsilon = 4.5 \times 10^3\text{ M}^{-1}\text{ cm}^{-1}$), 260 nm ($\epsilon = 5.6 \times 10^3\text{ M}^{-1}\text{ cm}^{-1}$), and 286 nm ($\epsilon = 3.1 \times 10^3\text{ M}^{-1}\text{ cm}^{-1}$), 441 nm ($\epsilon = 2 \times 10^2\text{ M}^{-1}\text{ cm}^{-1}$); UV–vis in methanol at 1 mM [Co] concentration: 238 ($\epsilon = 6.0 \times 10^3\text{ M}^{-1}\text{ cm}^{-1}$), 260 nm ($\epsilon = 1.0 \times 10^4\text{ M}^{-1}\text{ cm}^{-1}$), 540 nm ($1.0 \times 10^2\text{ M}^{-1}\text{ cm}^{-1}$). IR (cm^{-1}): 1609w, 1443w, 1283 m, 1154 m, 1027w, 922w, 828 s, 764 m, 652w, 554 s.

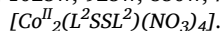
$[\text{Co}^{\text{II}}_2(\text{L}^1\text{SSL}^1)(\text{NO}_3)_4]$.

The ligand L^1SSL^1 (0.10 mmol; 51.7 mg) was dissolved in 5 mL dry and degassed acetonitrile, and then $\text{Co}(\text{NO}_3)_2 \cdot 6\text{H}_2\text{O}$ (0.20 mmol; 58.21 mg) was added, giving a dark red solution. After stirring for 1 h, 30 mL diethyl ether was added, resulting in a pink precipitate. The obtained precipitate was collected by filtration and washed with diethyl ether (2 \times 20 mL). Yield: 71.0 mg, 0.08 mmol, 81%. Single crystals suitable for X-ray diffraction were grown by vapor diffusion of diethyl ether into a methanolic solution of the compound. Elemental analysis calcd (%) for $\text{C}_{28}\text{H}_{32}\text{Co}_2\text{N}_{10}\text{O}_{12}\text{S}_2$: C 38.10, H 3.65, N 15.87; Found: C 38.17, H 3.74, N 15.81. ESI-MS in acetonitrile: found (calcd) for $\frac{1}{2}[\text{M}-2\text{NO}_3]^{2+}$ m/z 379.4 (379.3). UV–vis in acetonitrile at 1 mM [Co] concentration: 235 nm ($\epsilon = 7 \times 10^3\text{ M}^{-1}\text{ cm}^{-1}$), 261 nm ($\epsilon = 1 \times 10^4\text{ M}^{-1}\text{ cm}^{-1}$), 512 nm ($\epsilon = 2 \times 10^2\text{ M}^{-1}\text{ cm}^{-1}$); UV–vis in methanol at 1 mM [Co] concentration: 235 nm ($\epsilon = 6 \times 10^3\text{ M}^{-1}\text{ cm}^{-1}$), 261 nm ($\epsilon = 1 \times 10^4\text{ M}^{-1}\text{ cm}^{-1}$), 511 nm ($\epsilon = 2 \times 10^2\text{ M}^{-1}\text{ cm}^{-1}$). IR spectrum (cm^{-1}): 2971w, 1609 m, 1484 m, 1460 s, 1304 s, 1280 s, 1159w, 1102w, 1056w, 1023 s, 952w, 885w, 862w, 884w, 810w, 767 m, 736 w, 651w, 473w.

$[\text{Co}^{\text{II}}_2(\text{L}^2\text{SSL}^2)(\text{PO}_2\text{F}_2)_2](\text{PF}_6)_2$.

The ligand L^2SSL^2 (0.20 mmol; 108.1 mg) was dissolved in 5 mL dry

and degassed acetonitrile, and then CoCl_2 (0.40 mmol; 51.5 mg) was added, giving a dark purple solution. After stirring for 1 h, a purple suspension was obtained, to which AgPF_6 (0.80 mmol; 200.9 mg) and LiPO_2F_2 (0.40 mmol, 42.3 mg) were added, resulting in a pink solution with a white precipitate. The obtained mixture was stirred for 24 h and then filtered through celite, yielding a clear red solution. The obtained red solution was evaporated to 2 mL, to which 20 mL diethyl ether was added, which yielded a pink precipitate. The obtained precipitate was collected by filtration and washed with diethyl ether (3×15 mL). Single crystals suitable for synchrotron X-ray diffraction were grown by vapor diffusion of diethyl ether into an acetonitrile solution containing the compound. Yield: 119.0 mg, 0.10 mmol, 52%. Elemental analysis calcd for $\text{C}_{30}\text{H}_{36}\text{Co}_2\text{F}_{16}\text{N}_6\text{O}_4\text{P}_4\text{S}_2$: C 31.21, H 3.14, N 7.28; Found: C 31.17, H 3.09, N 7.21. ESI-MS in acetonitrile: found (calcd) for $[\frac{1}{2}[\text{M}-2\text{PF}_6]^{2+}] m/z$ 432.3 (432.1). UV-vis in acetonitrile at 2 mM [Co] concentration: 236 nm ($\epsilon = 5.0 \times 10^3 \text{ M}^{-1} \text{ cm}^{-1}$), 262 nm ($\epsilon = 1.0 \times 10^4 \text{ M}^{-1} \text{ cm}^{-1}$) and 510 nm ($\epsilon = 1.5 \times 10^2 \text{ M}^{-1} \text{ cm}^{-1}$). IR (cm^{-1}): 1610w, 1446w, 1307 m, 1160 m, 1023w, 923w, 830w, 766 m, 654w, 556 s.



The ligand L^2SSL^2 (0.10 mmol; 54.7 mg) was dissolved in 5 mL dry methanol, and then $\text{Co}(\text{NO}_3)_2 \cdot 6\text{H}_2\text{O}$ (0.20 mmol; 58.7 mg) was added, giving a dark red solution. After stirring for 1 h, 15 mL diethyl ether was added, resulting in a pink precipitate. The obtained precipitate was collected by filtration and washed with diethyl ether (2×10 mL). Yield: 32.0 mg, 0.04 mmol, 41%. Elemental analysis calcd (%) for $\text{C}_{30}\text{H}_{36}\text{Co}_2\text{N}_{10}\text{O}_{12}\text{S}_2$: C39.57, H 3.98, N 15.38; Found: C 39.54, H 3.95, N 15.24. ESI-MS in acetonitrile: found (calcd) for $[\frac{1}{2}[\text{M}-4\text{NO}_3 + 2\text{HCO}_2]^{2+}] m/z$ 376.3 (376.1). UV-vis in methanol at 1 mM [Co]: 235 nm ($\epsilon = 6.0 \times 10^3 \text{ M}^{-1} \text{ cm}^{-1}$), 263 nm ($\epsilon = 1.0 \times 10^4 \text{ M}^{-1} \text{ cm}^{-1}$), 510 nm ($\epsilon = 0.1 \times 10^3 \text{ M}^{-1} \text{ cm}^{-1}$). UV-vis in acetonitrile at 1 mM [Co]: 235 nm ($\epsilon = 6.0 \times 10^3 \text{ M}^{-1} \text{ cm}^{-1}$), 263 nm ($\epsilon = 1.0 \times 10^4 \text{ M}^{-1} \text{ cm}^{-1}$), 510 nm ($\epsilon = 0.2 \times 10^3 \text{ M}^{-1} \text{ cm}^{-1}$). IR (cm^{-1}): 1608 m, 1464 s, 1287 s, 1162w, 1093w, 1020 m, 768 m, 647w.

3. Results

3.1. Synthesis and characterization of Cobalt(II) compounds

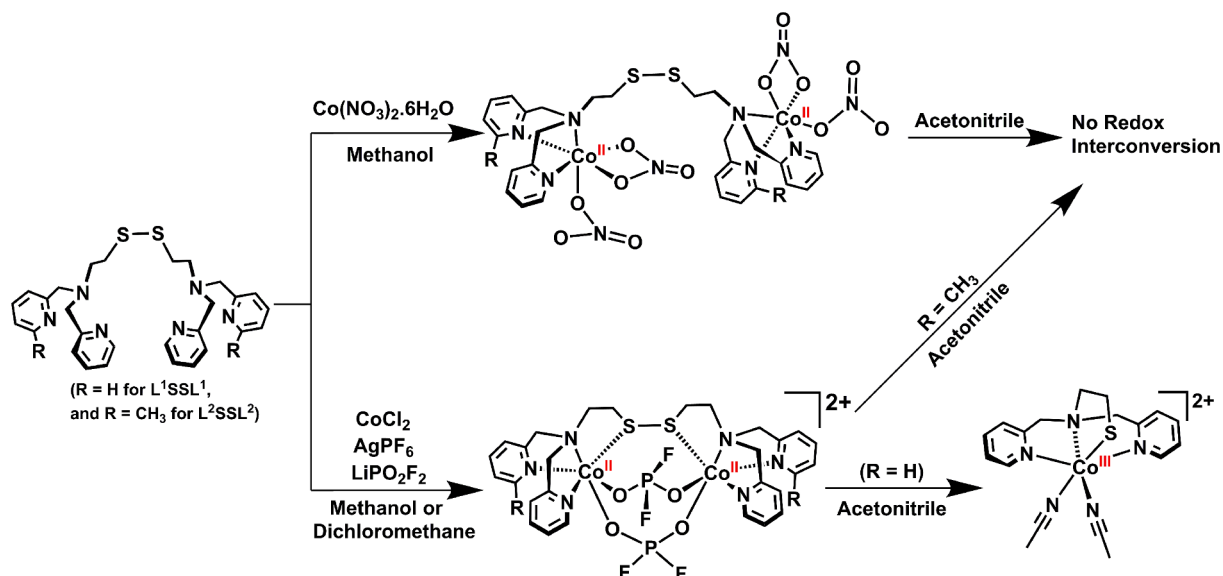
The ligands di-2-(bis(2-pyridylmethyl)amino)-ethyl disulfide (L^1SSL^1) and di-2-((6-methyl-2-pyridylmethyl)(2-pyridylmethyl)amino)-ethyl disulfide (L^2SSL^2) were synthesized using reported procedures [11,16]. Treatment of the ligand L^1SSL^1 with CoCl_2 and AgPF_6

in methanol resulted in a pink solution from which crystals of $[\text{Co}^{\text{II}}_2(\text{L}^1\text{SSL}^1)(\text{PO}_2\text{F}_2)_2](\text{PF}_6)_2$ were isolated (Scheme 1). The unexpected presence of the PO_2F_2^- anion was retraced to the use of an old batch of AgPF_6 that apparently was partly hydrolyzed. The compound was successfully reproduced in a yield of 30% using a 1:1 mixture of fresh AgPF_6 and commercially available LiPO_2F_2 [20]. Similarly, the compound $[\text{Co}^{\text{II}}_2(\text{L}^2\text{SSL}^2)(\text{PO}_2\text{F}_2)_2](\text{PF}_6)_2$ was first isolated starting from the old batch of AgPF_6 , but was reproduced in a yield of 52% using a mixture of AgPF_6 and LiPO_2F_2 . The addition of $\text{Co}(\text{NO}_3)_2 \cdot 6\text{H}_2\text{O}$ to a methanolic solution of the ligands L^1SSL^1 or L^2SSL^2 led to the formation of pink solutions from which the compounds $[\text{Co}^{\text{II}}_2(\text{L}^1\text{SSL}^1)(\text{NO}_3)_4]$ and $[\text{Co}^{\text{II}}_2(\text{L}^2\text{SSL}^2)(\text{NO}_3)_4]$ were isolated in a yield of 81% and 41%, respectively. The compounds were characterized by single crystal X-ray crystallography, electrospray ionization mass spectrometry (ESI-MS), elemental analysis, IR, UV-vis and nuclear magnetic resonance (NMR) spectroscopy.

3.2. Description of the crystal structures

Single crystals of $[\text{Co}^{\text{II}}_2(\text{L}^1\text{SSL}^1)(\text{PO}_2\text{F}_2)_2](\text{PF}_6)_2$, $[\text{Co}^{\text{II}}_2(\text{L}^1\text{SSL}^1)(\text{NO}_3)_4]$ and $[\text{Co}^{\text{II}}_2(\text{L}^2\text{SSL}^2)(\text{PO}_2\text{F}_2)_2](\text{PF}_6)_2$ suitable for X-ray structure determination were obtained by slow vapor diffusion of diethyl ether into solutions containing these compounds; experimental details of the data collection and refinement are provided in the Supporting Information (Table S1). Crystals of $[\text{Co}^{\text{II}}_2(\text{L}^1\text{SSL}^1)(\text{PO}_2\text{F}_2)_2](\text{PF}_6)_2$ were obtained from methanol as well as dichloromethane, but these are isomorphous as shown by X-ray diffraction. Projections of the structures of $[\text{Co}^{\text{II}}_2(\text{L}^1\text{SSL}^1)(\text{PO}_2\text{F}_2)_2](\text{PF}_6)_2$ and $[\text{Co}^{\text{II}}_2(\text{L}^1\text{SSL}^1)(\text{NO}_3)_4]$ are given in Fig. 1; a projection of the structure of $[\text{Co}^{\text{II}}_2(\text{L}^2\text{SSL}^2)(\text{PO}_2\text{F}_2)_2](\text{PF}_6)_2$ is provided in Fig. S1. Selected bond distances of all three compounds are provided in Table 1 and Table S2, selected bond angles for $[\text{Co}^{\text{II}}_2(\text{L}^1\text{SSL}^1)(\text{PO}_2\text{F}_2)_2](\text{PF}_6)_2$ and $[\text{Co}^{\text{II}}_2(\text{L}^1\text{SSL}^1)(\text{NO}_3)_4]$ are given in Table 2 and Table S3.

The compound $[\text{Co}^{\text{II}}_2(\text{L}^1\text{SSL}^1)(\text{PO}_2\text{F}_2)_2](\text{PF}_6)_2$ crystallizes in the triclinic space group $P\bar{1}$, with about 3.3 lattice solvent molecules of dichloromethane found in the asymmetric unit. The two Co(II) ions are each bound to three nitrogen donor atoms and one sulfur atom of the ligand and two oxygen atoms of separate difluoridophosphate anions in a distorted octahedral geometry. The three nitrogen donor atoms of the ligand are coordinated in a facial arrangement and the two difluoridophosphate ligands bridge between the two cobalt(II) metal centers. The Co-O bond lengths range from 2.0264(13) to 2.0991(13) Å, the



Scheme 1. Synthetic procedure of the cobalt(II)-disulfide compounds $[\text{Co}^{\text{II}}_2(\text{L}^x\text{SSL}^x)(\text{NO}_3)_4]$ and $[\text{Co}^{\text{II}}_2(\text{L}^x\text{SSL}^x)(\text{PO}_2\text{F}_2)_2](\text{PF}_6)_2$ and their reactivity in acetonitrile.

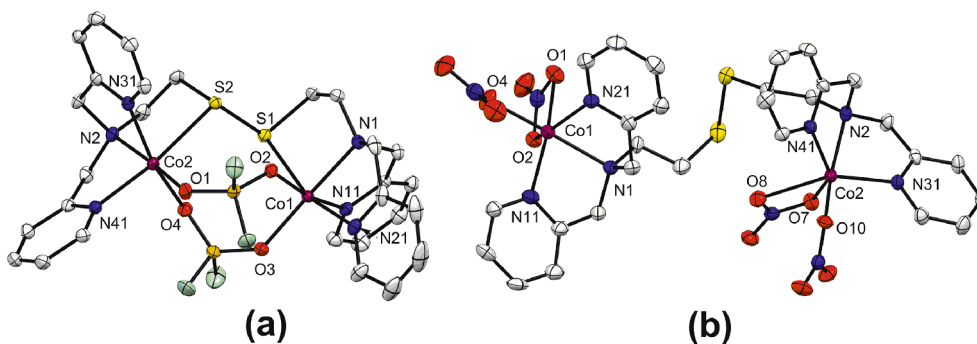


Fig. 1. Displacement ellipsoid plot (50% probability level) of (a) the cationic part of $[\text{Co}^{\text{II}}_2(\text{L}^1\text{SSL}^1)(\text{PO}_2\text{F}_2)_2](\text{PF}_6)_2$ and (b) $[\text{Co}^{\text{II}}_2(\text{L}^1\text{SSL}^1)(\text{NO}_3)_4]$ at 110(2) K. Disorder, lattice solvent molecules, non-coordinating PF_6 anions (for a) and hydrogen atoms are omitted for clarity.

Table 1

Selected bond distances (Å) from the structures of the compounds $[\text{Co}^{\text{II}}_2(\text{L}^1\text{SSL}^1)(\text{PO}_2\text{F}_2)_2](\text{PF}_6)_2$, $[\text{Co}^{\text{II}}_2(\text{L}^2\text{SSL}^2)(\text{PO}_2\text{F}_2)_2](\text{PF}_6)_2$ and $[\text{Co}^{\text{II}}_2(\text{L}^1\text{SSL}^1)(\text{NO}_3)_4]$.

Bond lengths	$[\text{Co}^{\text{II}}_2(\text{L}^1\text{SSL}^1)(\text{PO}_2\text{F}_2)_2](\text{PF}_6)_2$	$[\text{Co}^{\text{II}}_2(\text{L}^2\text{SSL}^2)(\text{PO}_2\text{F}_2)_2](\text{PF}_6)_2$	$[\text{Co}^{\text{II}}_2(\text{L}^1\text{SSL}^1)(\text{NO}_3)_4]$
Co1-N1	2.1405(15)	2.139(4)	2.214(3)
Co1-N11	2.1038(15)	2.124(5)	2.085(3)
Co1-N21	2.0797(15)	2.077(5)	2.091(3)
Co1-X1	2.5927(5)	2.7119(16)	2.125(2)
Co1-X2	2.0991(13)	2.057(4)	2.333(3)
Co1-X3	2.0264(13)	2.043(4)	2.071(3)
S1-S2	2.0531(6)	2.052(3)	2.0372(14)

(X1 = S1, X2 = O2, X3 = O3 for $[\text{Co}^{\text{II}}_2(\text{L}^1\text{SSL}^1)(\text{PO}_2\text{F}_2)_2](\text{PF}_6)_2$; X1 = S1, X2 = O2, X3 = O1 for $[\text{Co}^{\text{II}}_2(\text{L}^2\text{SSL}^2)(\text{PO}_2\text{F}_2)_2](\text{PF}_6)_2$; X1 = O1, X2 = O2, X3 = O4 for $[\text{Co}^{\text{II}}_2(\text{L}^1\text{SSL}^1)(\text{NO}_3)_4]$)

Table 2

Selected bond angles (°) in the structures of $[\text{Co}^{\text{II}}_2(\text{L}^1\text{SSL}^1)(\text{PO}_2\text{F}_2)_2](\text{PF}_6)_2$ and $[\text{Co}^{\text{II}}_2(\text{L}^1\text{SSL}^1)(\text{NO}_3)_4]$.

Bond angles	$[\text{Co}^{\text{II}}_2(\text{L}^1\text{SSL}^1)(\text{PO}_2\text{F}_2)_2](\text{PF}_6)_2$	Bond angles	$[\text{Co}^{\text{II}}_2(\text{L}^1\text{SSL}^1)(\text{NO}_3)_4]$
S1-Co1-O2	86.65(4)	N1-Co1-N11	77.84(11)
S1-Co1-O3	99.59(4)	N1-Co1-N21	76.91(11)
S1-Co1-N1	84.93(4)	N1-Co1-O1	88.13(10)
S1-Co1-N11	79.11(4)	N1-Co1-O2	100.55(10)
S1-Co1-N21	163.91(5)	N1-Co1-O4	174.11(11)
O2-Co1-O3	94.19(5)	N11-Co1-N21	115.97(12)
O2-Co1-N1	90.65(6)	N11-Co1-O1	93.75(11)
O2-Co1-N11	163.53(6)	N11-Co1-O2	150.89(11)
O2-Co1-N21	89.57(5)	N11-Co1-O4	102.20(12)
O3-Co1-N1	173.55(6)	N21-Co1-O1	142.27(11)
O3-Co1-N11	96.28(6)	N21-Co1-O2	91.40(10)
O3-Co1-N21	96.28(6)	N21-Co1-O4	108.08(12)
N1-Co1-N11	79.97(6)	O1-Co1-O2	57.18(9)
N1-Co1-N21	79.48(6)	O1-Co1-O4	85.99(11)
N11-Co1-N21	101.84(6)	O2-Co1-O4	76.50(10)

Co-S bond lengths are 2.5927(5) and 2.6190(5) Å. The Co-N bond distances range from 2.0797(15) to 2.1405(15) Å, and the S-S bond length is 2.0531(6) Å. The compound $[\text{Co}^{\text{II}}_2(\text{L}^2\text{SSL}^2)(\text{PO}_2\text{F}_2)_2](\text{PF}_6)_2$ crystallizes in the monoclinic space group $P2_1/n$, with diethyl ether co-crystallized in the asymmetric unit. The structure is highly similar to that of $[\text{Co}^{\text{II}}_2(\text{L}^1\text{SSL}^1)(\text{PO}_2\text{F}_2)_2](\text{PF}_6)_2$. The slightly longer Co1-N11 distance might be a result of steric hindrance caused by the presence of the methyl group *ortho* to the pyridine nitrogen atom [22].

The compound $[\text{Co}^{\text{II}}_2(\text{L}^1\text{SSL}^1)(\text{NO}_3)_4]$ crystallizes in the monoclinic space group $P2_1/n$. Both Co(II) ions are coordinated by three nitrogen donors of the ligand and three oxygen atoms of one monodentate and one bidentate nitrate anion. Although the cobalt centers in

$[\text{Co}^{\text{II}}_2(\text{L}^1\text{SSL}^1)(\text{NO}_3)_4]$ are surrounded by six donor atoms, the coordination geometry of the cobalt centers is best described as distorted trigonal-bipyramidal, considering the two coordinated oxygen atoms from the bidentate nitrate ligand to occupy one coordination site. The Co-O and Co-N bond distances range from 2.071(3) to 2.354(2) Å, and from 2.060(3) to 2.249(3) Å, respectively. The disulfide sulfur atoms are non-coordinating and the S-S bond length is 2.0372(14) Å, which is slightly shorter than in $[\text{Co}^{\text{II}}_2(\text{L}^1\text{SSL}^1)(\text{PO}_2\text{F}_2)_2](\text{PF}_6)_2$. Stacking interactions are not present in the structures, despite the presence of the aromatic pyridine groups.

3.3. Characterization and solution studies of the Cobalt(II) compounds

The compound $[\text{Co}^{\text{II}}_2(\text{L}^1\text{SSL}^1)(\text{PO}_2\text{F}_2)_2](\text{PF}_6)_2$ dissolved in acetonitrile gives a yellow-colored solution, whereas solutions in methanol or dichloromethane are pink. Solutions of methylated $[\text{Co}^{\text{II}}_2(\text{L}^2\text{SSL}^2)(\text{PO}_2\text{F}_2)_2](\text{PF}_6)_2$ are colored pink, both in acetonitrile and methanol. ^1H NMR spectra were recorded for solutions of $[\text{Co}^{\text{II}}_2(\text{L}^1\text{SSL}^1)(\text{PO}_2\text{F}_2)_2](\text{PF}_6)_2$ in acetonitrile- d_3 , methanol- d_4 and dichloromethane- d_2 (Figs. S2, S3, S4). The NMR spectra in dichloromethane- d_2 and methanol- d_4 show large downfield shifts up to around 70 ppm typical for a paramagnetic compound, whereas the spectrum in acetonitrile shows resonances in the diamagnetic region, indicating the presence of a low-spin cobalt(III) ion ($S = 0$); this spectrum is identical to the one earlier reported for $[\text{Co}(\text{L}^1\text{S})(\text{MeCN})_2]^{2+}$ [18]. In contrast, ^1H NMR spectra of the methylated compound $[\text{Co}^{\text{II}}_2(\text{L}^2\text{SSL}^2)(\text{PO}_2\text{F}_2)_2](\text{PF}_6)_2$ in acetonitrile- d_3 shows that the compound is paramagnetic (Fig. S5). The effective magnetic moment of $[\text{Co}^{\text{II}}_2(\text{L}^1\text{SSL}^1)(\text{PO}_2\text{F}_2)_2](\text{PF}_6)_2$ dissolved in methanol as well as for the related compound with L^2SSL^2 in acetonitrile were estimated using Evan's method, resulting in values for μ_{eff} of 6.56 μ_{B} and 6.59 μ_{B} , respectively, both consistent with the presence of two high-spin ($S = 3/2$) cobalt(II) centers.

The UV-vis spectra of the solid samples of $[\text{Co}^{\text{II}}_2(\text{L}^1\text{SSL}^1)(\text{PO}_2\text{F}_2)_2](\text{PF}_6)_2$ and $[\text{Co}^{\text{II}}_2(\text{L}^2\text{SSL}^2)(\text{PO}_2\text{F}_2)_2](\text{PF}_6)_2$ show absorption bands at 254, 456, 501, 545 and approximately 1100 nm; the observed *d-d* transitions are in agreement with cobalt(II) centers in an octahedral geometry (Figs. S6, S7) [23]. The UV-vis spectrum of $[\text{Co}^{\text{II}}_2(\text{L}^1\text{SSL}^1)(\text{PO}_2\text{F}_2)_2](\text{PF}_6)_2$ dissolved in acetonitrile resembles that of the compound $[\text{Co}^{\text{II}}(\text{L}^1\text{S})(\text{MeCN})_2](\text{BF}_4)_2$ reported in our previous study, showing absorption bands at 240, 260, 285 and 440 nm (Fig. 2) [18]. The peaks at 240 and 260 nm are ascribed to $\pi^* \leftarrow \pi$ transitions of the pyridyl groups, and the peaks at 285 and 440 nm are tentatively ascribed to Co \leftarrow S charge-transfer transitions (LMCT) [24]. In methanolic solution two peaks are observed at 238 ($\epsilon = 6.0 \times 10^3 \text{ M}^{-1}\text{cm}^{-1}$) and 260 nm ($\epsilon = 1.0 \times 10^4 \text{ M}^{-1}\text{cm}^{-1}$), attributed to $\pi^* \leftarrow \pi$ transitions of the pyridyl groups; another featureless peak at 540 nm ($\epsilon = 1 \times 10^2 \text{ M}^{-1}\text{cm}^{-1}$) is ascribed to a *d-d* transition [23]. The UV-vis spectra of the methylated compound $[\text{Co}^{\text{II}}_2(\text{L}^2\text{SSL}^2)(\text{PO}_2\text{F}_2)_2](\text{PF}_6)_2$ both in acetonitrile and in methanol show absorption bands at 236 nm ($\epsilon = 5.0 \times 10^3 \text{ M}^{-1}\text{cm}^{-1}$) and 262 nm ($\epsilon = 1.0 \times 10^4 \text{ M}^{-1}\text{cm}^{-1}$) corresponding to $\pi^* \leftarrow \pi$ transition of the

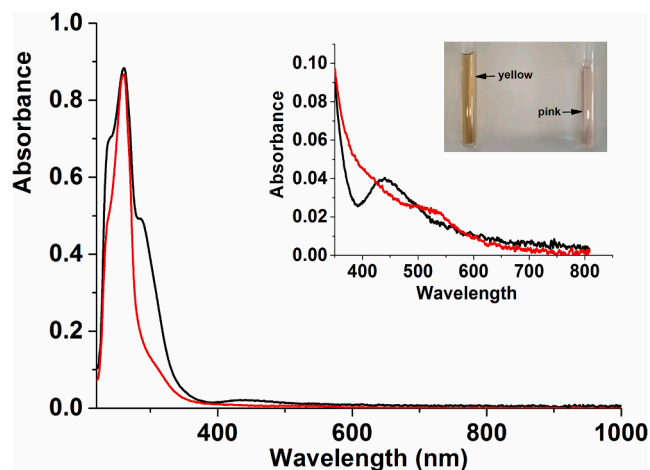


Fig. 2. UV-vis spectra of the compound $[\text{Co}^{\text{II}}_2(\text{L}^1\text{SSL}^1)(\text{PO}_2\text{F}_2)_2](\text{PF}_6)_2$ dissolved in methanol (pink solution, red line) and in acetonitrile (yellow solution, black line); UV-vis spectra were recorded using solutions 1 mM [Co] (0.5 mM of the dinuclear compound) with a transmission dip probe path length of 1.8 mm. The inset shows the UV-vis spectra of 2.2 mM [Co] in acetonitrile (black) and 4.4 mM [Co] in methanol (red).

pyridyl groups. The weak featureless band at 510 nm ($\epsilon = 0.2 \times 10^3 \text{ M}^{-1}\text{cm}^{-1}$) observed for $[\text{Co}^{\text{II}}_2(\text{L}^2\text{SSL}^2)(\text{PO}_2\text{F}_2)_2](\text{PF}_6)_2$ in acetonitrile is ascribed to a $d-d$ transition of the cobalt(II) ions (Fig. S8) [23]. The significant red-shift of the $d-d$ transition in the spectra recorded in methanol compared to those in acetonitrile indicate that in solution the PO_2F_2^- anions are replaced by the solvent; the higher-energy band in acetonitrile is in agreement with the ligand-field strength of acetonitrile being larger than that of methanol.

Titration of small amounts of dichloromethane into a solution of $[\text{Co}^{\text{II}}_2(\text{L}^1\text{SSL}^1)(\text{PO}_2\text{F}_2)_2](\text{PF}_6)_2$ in acetonitrile resulted in changes in the UV-vis spectra that are mainly caused by dilution of the solution rather than the gradual formation of a Co(II) disulfide compound (Fig. S9). The use of different ratios of acetonitrile and dichloromethane solutions of $[\text{Co}^{\text{II}}_2(\text{L}^1\text{SSL}^1)(\text{PO}_2\text{F}_2)_2](\text{PF}_6)_2$ also does not result in significant differences in UV-vis spectra, except for the disappearance of the band at 285 nm typical for the cobalt(III) thiolate compound (Fig. S10).

ESI-MS spectra of $[\text{Co}^{\text{II}}_2(\text{L}^1\text{SSL}^1)(\text{PO}_2\text{F}_2)_2](\text{PF}_6)_2$ dissolved in acetonitrile present a dominant peak at m/z 199.5, fitting the fragment $[\text{Co}(\text{L}^1\text{S})(\text{MeCN})_2]^{2+}$ (Fig. S11). The spectroscopic evidence in combination with the knowledge obtained in our previous study thus indicates that the cobalt(II)-disulfide compound $[\text{Co}^{\text{II}}_2(\text{L}^1\text{SSL}^1)(\text{PO}_2\text{F}_2)_2](\text{PF}_6)_2$ is stable as such in methanol or dichloromethane solutions, but undergoes redox conversion to the cobalt(III)-thiolate compound $[\text{Co}^{\text{III}}(\text{L}^1\text{S})(\text{MeCN})_2]^{2+}$ when dissolved in acetonitrile. The ESI-MS spectrum of a solution of the compound in acetonitrile reveals a peak at m/z 432.3 ascribed to the dicationic species $[\text{Co}^{\text{II}}_2(\text{L}^2\text{SSL}^2)(\text{PO}_2\text{F}_2)_2]^{2+}$ (Fig. S12). The obtained results thus suggest that, in contrast to the non-methylated compound comprising ligand L^1SSL^1 , the compound $[\text{Co}^{\text{II}}_2(\text{L}^2\text{SSL}^2)(\text{PO}_2\text{F}_2)_2](\text{PF}_6)_2$ is stable as such in methanol as well as acetonitrile.

The UV-vis spectrum of a solid sample of $[\text{Co}^{\text{II}}_2(\text{L}^1\text{SSL}^1)(\text{NO}_3)_4]$ reveals absorption bands at 260, 385 nm, as well as a broad band between 460 and 540 nm and rather weak features at 680 and approximately 1000 nm (Fig. S13); UV-vis spectra of solid $[\text{Co}^{\text{II}}_2(\text{L}^2\text{SSL}^2)(\text{NO}_3)_4]$ are rather similar (Fig. S14). The solid-state spectra of the nitrate compounds do not clearly indicate an octahedral geometry of the cobalt(II) centers, in agreement with the distorted geometries observed in the crystal structure.

Solutions of $[\text{Co}^{\text{II}}_2(\text{L}^1\text{SSL}^1)(\text{NO}_3)_4]$ and $[\text{Co}^{\text{II}}_2(\text{L}^2\text{SSL}^2)(\text{NO}_3)_4]$ are colored pink, both in acetonitrile and methanol. UV-vis spectra of the compounds in acetonitrile show absorption bands at 235 nm ($\epsilon = 7 \times 10^3 \text{ M}^{-1}\text{cm}^{-1}$) and 261 nm ($\epsilon = 1 \times 10^4 \text{ M}^{-1}\text{cm}^{-1}$), corresponding to

$\pi^* \leftarrow \pi$ transition of the pyridyl groups, and a weak, featureless band at 510 nm ($\epsilon = 0.2 \times 10^3 \text{ M}^{-1}\text{cm}^{-1}$) arising from a $d-d$ transition of the cobalt(II) ions (Figs. S15, S16) [23]. UV-vis spectra in methanol show similar features. The lack of a sulfur-to-cobalt LMCT transition and the pink color of the solutions indicate the presence of a Co(II)-disulfide compound in both solvents. The $d-d$ transitions appear at exactly the same wavelength in methanol and acetonitrile indicating that the nitrate ions are not replaced by solvent molecules, in contrast with the finding for the compounds containing the PO_2F_2^- anion. ^1H NMR spectra of the compounds dissolved in acetonitrile- d_3 or methanol- d_4 show downfield shifts up to around 90 ppm (Figs. S17, S18, S19). The ESI-MS spectra of the compounds in acetonitrile show peaks at m/z 379.4 for the species $[\text{Co}^{\text{II}}_2(\text{L}^1\text{SSL}^1)(\text{NO}_3)_2]^{2+}$ and m/z 376.3 for the dicationic species $[\text{Co}^{\text{II}}_2(\text{L}^2\text{SSL}^2)(\text{HCO}_2)_2]^{2+}$, respectively (Figs. S20, S21). The obtained results suggest that the nitrate compounds $[\text{Co}^{\text{II}}_2(\text{L}^1\text{SSL}^1)(\text{NO}_3)_4]$ and $[\text{Co}^{\text{II}}_2(\text{L}^2\text{SSL}^2)(\text{NO}_3)_4]$ are stable as such both in coordinating and non-coordinating solvents.

4. Discussion

In the last decade, the redox interconversion reaction has been extensively studied for copper compounds based on the ligand scaffold L^1SSL^1 . In recent years the group of Duboc expanded the study of redox isomerization to other transition metals, notably cobalt, manganese and iron, using another ligand set [17,19,25]. The chemistry of redox interconversion appears to be rather complex, as different results are obtained upon subtle changes in the ligand systems, and depend on the choice of metal ion, anions or solvents.

Different results are obtained when the ligand L^1SSL^1 is used in combination with cobalt(II) instead of copper(I) salts. The presence of coordinating chloride ions induces the formation of the cobalt(II)-disulfide compound, analogous to the result with copper [18]. However, in contrast to copper, the cobalt(III)-thiolate species is favored in acetonitrile solutions in combination with non-coordinating anions. Thus, for the ligand L^1SSL^1 the use of tetrafluoroborate or difluoridophosphate anions in acetonitrile leads to the formation of the cobalt(III)-thiolate species $[\text{Co}(\text{L}^1\text{S})(\text{MeCN})_2]^{2+}$. Yet, the matter is even more complicated, as use of the coordinating thiocyanate anion in combination with L^1SSL^1 leads to the formation of $[\text{Co}^{\text{III}}(\text{L}^1\text{S})(\text{NCS})_2]$, not only in acetonitrile [18], but also in methanol or acetone (Fig. S22).

It seems that for the ligand system based on the L^1SSL^1 scaffold, the formation of the copper(II)-thiolate redox isomer is mainly dictated by the coordination strength of the anion or the solvent: coordinating anions (Cl^-) or solvents (acetonitrile) lead to the formation of the copper(I) disulfide compounds. In contrast, with the same ligand scaffold the formation of the cobalt(III) thiolate compound seems to be related to the ligand-field strength of the anion or solvent, in combination with their relative coordination strength. Ligands (solvent or anion) inducing a large ligand-field splitting initially may result in the formation of a low-spin cobalt(II)-disulfide compound with one single electron in a high-energy orbital and a 19-electron count. It is plausible that this low-spin state results in redox isomerization to form the low-spin cobalt(III)-thiolate compound, as then a stable compound is formed with an 18-electron count. Thus, for the ligand L^1SSL^1 in combination with cobalt(II) ions weakly coordinating anions (BF_4^- , PO_2F_2^-) in acetonitrile (coordinating and relatively strong ligand field) lead to the formation of $[\text{Co}^{\text{III}}(\text{L}^1\text{S})(\text{MeCN})_2]^{2+}$, whereas acetonitrile is not able to replace the anions Cl^- and NO_3^- (strongly binding and weaker ligand field). In agreement with this reasoning, the strongly binding NCS^- anion gives rise to a larger ligand-field splitting than Cl^- or NO_3^- , and thus results in the formation of $[\text{Co}^{\text{III}}(\text{L}^1\text{S})(\text{NCS})_2]$ [18], regardless of the solvent used.

The ligand-field splitting caused by the ligand L^2SSL^2 apparently is smaller than that of L^1SSL^1 , based on the observation that replacement of the PO_2F_2^- anions by acetonitrile is not sufficient to lead to a low-spin state of the cobalt(II) center and subsequent electron transfer. Even in combination with strong-field thiocyanate ions the disulfide compound

$[\text{Co}^{\text{II}}_2(\text{L}^2\text{SSL}^2)(\text{NCS})_4]$ is obtained (Figs. S23-S25). The smaller ligand-field splitting of L^2SSL^2 may be due to the steric hindrance caused by the two methyl groups, causing a decrease in the donor ability of the methylated pyridine rings as indicated by the slightly longer Co – N bond distances.

5. Conclusions

We have described the synthesis and characterization of four new cobalt(II) disulfide compounds, based on the ligands L^1SSL^1 and L^2SSL^2 , and using the anions PO_2F_2^- and NO_3^- . It is shown that a coordinating solvent such as acetonitrile induces redox conversion of $[\text{Co}^{\text{II}}_2(\text{L}^1\text{SSL}^1)(\text{PO}_2\text{F}_2)_2](\text{PF}_6)_2$, forming the cobalt(III)-thiolate compound $[\text{Co}^{\text{III}}(\text{L}^1\text{S})(\text{MeCN})_2]^{2+}$, whereas this does not occur for $[\text{Co}^{\text{II}}_2(\text{L}^1\text{SSL}^1)(\text{NO}_3)_4]$. The cobalt(II) compounds of the related ligand L^2SSL^2 , in which methyl groups are present at two of the pyridine rings, does not show redox conversion in any of the investigated solvents.

The results indicate that for ligands based on the L^1SSL^1 scaffold formation of the cobalt(III) thiolate is triggered by ligands that induce larger ligand-field splitting, in combination with the relative coordination strengths of ligands, solvents and anions. Future experimental and computational studies will be directed to generate further understanding of the factors influencing the redox isomerization of cobalt compounds of disulfide ligands.

CRedit authorship contribution statement

Feng Jiang: Investigation, Formal analysis, Writing – original draft. **Christian Marvelous:** Validation, Formal analysis. **Amaya C. Verschuur:** Investigation, Formal analysis. **Maxime A. Siegler:** Resources, Formal analysis, Writing – review & editing. **Simon J. Teat:** Resources. **Elisabeth Bouwman:** Conceptualization, Resources, Writing – review & editing, Supervision, Project administration, Funding acquisition.

Declaration of Competing Interest

The authors declare that they have no known competing financial interests or personal relationships that could have appeared to influence the work reported in this paper.

Acknowledgments

FJ gratefully acknowledges the China Scholarship Council (CSC) for a personal grant (No.201406890012). We thank Dr. Sipeng Zheng for

ESI-MS analysis and Mr. Fons Lefeber for assistance with the NMR spectrometers. Dr. José Sanchez Costa (IMDEA-Nanoscience, Madrid, Spain) is acknowledged for his help with the collection and processing of synchrotron data for one of the structures.

Appendix A. Supplementary data

Supplementary data to this article can be found online at <https://doi.org/10.1016/j.ica.2022.120880>.

References

- [1] H.F. Gilbert, *Methods Enzymol.* 251 (1995) 8–28.
- [2] C. Jacob, G.I. Giles, N.M. Giles, H. Sies, *Angew. Chem., Int. Edit.* 42 (2003) 4742–4758.
- [3] R. Singh, G.M. Whitesides, Thiol-disulfide interchange, in: *Sulphur-containing functional groups*, John Wiley & Sons, Inc.: Chichester, UK, 1993, pp. 633–658.
- [4] E.I. Solomon, U.M. Sundaram, T.E. Machonkin, *Chem. Rev.* 96 (1996) 2563–2606.
- [5] X.Q. Zhou, I. Carbo-Bague, M.A. Siegler, J. Hilgendorf, U. Basu, I. Ott, R.F. Liu, L.Y. Zhang, V. Ramu, A.P. IJerman, S. Bonnet, *JACS Au*, 1 (2021) 380–395.
- [6] A. Santoro, J.S. Calvo, M.D. Peris-Diaz, A. Krezel, G. Meloni, P. Faller, *Angew. Chem., Int. Edit.* 59 (2020) 7830–7835.
- [7] M.V. Palmeira-Mello, A.B. Caballero, J.M. Ribeiro, E.M. de Souza-Fagundes, P. Gamez, M. Lanznaster, *J. Inorg. Biochem.* 211 (2020), 111211.
- [8] G. Meloni, P. Faller, M. Vasak, *J. Biol. Chem.* 282 (2007) 16068–16078.
- [9] G. Meloni, V. Sonois, T. Delaine, L. Guilloureau, A. Gillet, J. Teissie, P. Faller, M. Vašák, *Nat. Chem. Biol.* 4 (2008) 366–372.
- [10] J.T. Pedersen, C. Hureau, L. Hemmingsen, N.H. Heegaard, J. Østergaard, M. Vašák, P. Faller, *Biochemistry* 51 (2012) 1697–1706.
- [11] S. Itoh, M. Nagagawa, S. Fukuzumi, *J. Am. Chem. Soc.* 123 (2001) 4087–4088.
- [12] A. Neuba, R. Haase, W. Meyer-Klaucke, U. Flörke, G. Henkel, *Angew. Chem., Int. Edit.* 51 (2012) 1714–1718.
- [13] E. Ording-Wenker, M. van der Plas, M.A. Siegler, C. Fonseca Guerra, E. Bouwman, *Chem. Eur. J.* 20 (2014) 16913–16921.
- [14] E.C. Ording-Wenker, M. van der Plas, M.A. Siegler, S. Bonnet, F.M. Bickelhaupt, C. Fonseca Guerra, E. Bouwman, *Inorg. Chem.* 53 (2014) 8494–8504.
- [15] A.M. Thomas, B.-L. Lin, E.C. Wasinger, T.D.P. Stack, *J. Am. Chem. Soc.* 135 (2013) 18912–18919.
- [16] Y. Ueno, Y. Tachi, S. Itoh, *J. Am. Chem. Soc.* 124 (2002) 12428–12429.
- [17] M. Gennari, B. Gerey, N. Hall, J. Pécaut, M.N. Collomb, M. Rouzières, R. Clérac, M. Orio, C. Duboc, *Angew. Chem., Int. Edit.* 53 (2014) 5318–5321.
- [18] F. Jiang, M.A. Siegler, X. Sun, L. Jiang, C. Fonseca Guerra, E. Bouwman, *Inorg. Chem.* 57 (2018) 8796.
- [19] L. Wang, F.G. Cantú Reinhard, C. Philouze, S. Demeshko, S.P. de Visser, F. Meyer, M. Gennari, C. Duboc, *Chem. Eur. J.* 24 (2018) 11973.
- [20] The chemical LiPO_2F_2 was purchased from <http://www.chemfish.com/>.
- [21] G.M. Sheldrick, *Acta Cryst. C Struct. Chem.* 71 (2015) 3–8.
- [22] H. Nagao, N. Komeda, M. Mukaida, M. Suzuki, K. Tanaka, *Inorg. Chem.* 35 (1996) 6809–6815.
- [23] A.B.P. Lever, *Inorganic Electronic Spectroscopy*, second ed., Elsevier, 1968.
- [24] I.K. Adzamlı, K. Libson, J. Lydon, R. Elder, E. Deutsch, *Inorg. Chem.* 18 (1979) 303–311.
- [25] M. Gennari, D. Brazzolotto, S. Yu, J. Pécaut, C. Philouze, M. Rouzières, R. Clérac, M. Orio, C. Duboc, *Chem. Eur. J.* 21 (2015) 18770–18778.